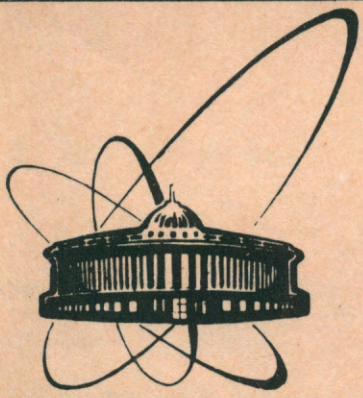

объединенный
институт
ядерных
исследований
дубна

E4-91-314

S.N.Belyaev*, O.V.Vasiliev*, V.V.Voronov,
A.A.Nechkin*, V.Yu.Ponomarev, V.A.Semenov*

STRUCTURES OF THE (γ, n) ^{208}Pb CROSS SECTION

Submitted to "Ядерная физика"

*Research Institute for Mechanics and Physics
of Saratov State University, USSR

1991

1 Introduction

A lot of information has been obtained on the properties of multipole giant resonances from studies of different nuclear reactions [1–3]. The photonuclear reaction is one of the most effective tools to study the giant dipole resonance (GDR) properties. Improving the energy resolution one expect hopes to obtain new information on the GDR fine structure [4,5]. In particular, substructures in the (γ, n) cross sections at low excitation energies have been observed [4–6].

The existence of substructures of that type in semimagic nuclei have been discussed in [7]. The theoretical studies [7–13] of giant resonances lead to a conclusion that the giant resonance damping is caused by the coupling of simple nuclear particle-hole configurations with the complex ones. There is a relatively weak coupling between these configurations in nuclei near closed shells, and as a result, substructures appear at low excitation energies where the level density is much lower than in the GDR maximum region [7].

The aim of this paper is to investigate the substructures in the photon absorption cross sections of ^{208}Pb and to compare experimental data with the calculations within the quasiparticle phonon nuclear model (QPM) [14–16].

2 Experimental technique and apparatus

Photoneutron cross sections in ^{208}Pb w[illegible] measured by means of bremsstrahlung radiation of a betatron with the maximum endpoint energy equal to 25 MeV. The reliability of the results with this technique depends on the following:

1). on the possibility of the long duration stability of the running accelerator and apparatus parameters within the required experimental boundaries;

2). on a choice of a method of obtaining experimental cross sections from the measured photoneutron yield by solving the inverse scattering problem.

Using the multichannel method [17] and achieving the accuracy of the endpoint energy $E_{\gamma max}$ as 5 keV [18] one can perform measurements with a small energy step and large statistics to obtain a good level resolution. As model calculations with the input data close to real the ones show, the energy step of 50 keV allows one to reveal structures in the cross section with the width about 150 – 200 keV. The smoothing of the neutron yield curve comes from the uncertainty of the endpoint energy $E_{\gamma max}$ caused by the electron beam displacement time on the accelerator target which is about 25 – 30 keV for the electrons at 25 MeV. The energy scale calibration was performed at the photoneutron threshold and by the break of neutron yield curve in ^{16}O at 17.25 MeV with the uncertainty of 20 keV.

The moderated neutrons were detected by $^{10}BF_3$ – counters with the summary efficiency of somewhat 20% [19]. The influence on the results of the gamma – ray intensity fluctuation was suppressed by normalization of detected neutrons on the number of gammas measured by scintillation dosimeter [20] for every gamma – pulse. All data were controlled by visual monitoring on a graphical display.

Our previous measurements of the (γ,n) cross section on ^{208}Pb were performed with the step 25 keV up to the excitation energy of 9 MeV and with the step 50 keV up to 12 MeV [5]. In this paper, we present results covering the excitation energy from the photoneutron threshold B_n up to 22 MeV with a different step of $E_{\gamma max}$. This step is equal to 40 keV for the range of $E_{\gamma max}$ from the B_n up to 8.5 MeV, to 60 keV for the $E_{\gamma max}$ up to 12 MeV and to

120 keV for the $E_{\gamma max}$ up to 22 MeV. A small step of $E_{\gamma max}$ at low energies was chosen to compensate a small neutron yield near the threshold by a larger number of measurements at these energies. The same target with the thickness 2.52 g/cm^2 and the enrichment 99% was used for all measurements.

As a result of measurements we obtained a sample mean of a neutrons yield and a sample standard deviation at chosen values of $E_{\gamma max}$. Taking into account the background corrections and counting errors and reducing the yield values on dose units, one can use data for the extraction of the (γ,n) cross section.

3 Extraction of the (γ,n) cross section from the photoneutron yield

With the bremsstrahlung technique the (γ,n) cross section is obtained as a solution of the set of integral equations of the inverse scattering problem

$$\int_{B_n}^{E^i_{\gamma max}} \Phi(E^i_{\gamma max}, E^i_\gamma)\, \sigma_{exp}(E\gamma) dE_\gamma = Y(E^i_{\gamma max}) \qquad (1)$$

where $\Phi(E^i_{\gamma max})$ is a bremsstrahlung spectrum, $Y(E^i_{\gamma max})$ is a reduced photoneutron yield, $\sigma(E\gamma)$ is an experimental (γ,n) cross section practically equal to the sum $\sigma(\gamma,n) + \sigma(\gamma,2n)$ due to a small contribution of other partial reactions.

Since the input data of Eq. (1) are obtained with some uncertainties (being estimations on a limited sampling) we can get only an approximate solution of this set of equations. It may vary strongly with small variations of input data; thus, this problem belongs to the ill–posed unfolding problems. In the present paper, the statistical regularization method [21] to obtain cross sections was

used. This method is based on the Bayessian approach and the probability nature of experimental data is used. In our case, the measured yield values $Y(E^i_{\gamma max})$ are mean values with respect to a random variable sampling, and therefore, these values are also stochastic variables and their deviations from true values may be given by a distribution law. Here, we assume that it is the normal distribution with the variance equal to the variance of our experimental data which is in our case is a variance of a photoneutron yield.

A solution of Eq.(1) is searched on the smooth function ensemble which belongs to some distribution. The density of this distribution is determined as a posterior probability density of a solution σ by given values of Y:

$$P(\sigma/Y) = P(\sigma)\,P(Y/\sigma) \qquad (2)$$

where $P(\sigma)$ is a prior probability density determined under the conditions of information minimum and smoothness of a solution, and $P(Y/\sigma)$ is a conditional probability density of a given value of Y under the condition that σ exists.

The solution σ is obtained by the method of maximum of a posterior probability density, while its uncertainty $\Delta\sigma$ is the standard deviation of this distribution. This method allows one to process the data obtained with a nonconstant step of the endpoint energy $E_{\gamma max}$ and to take into account a weight of every yield point.

In this approach no false structures appear in a cross section. It is known that the initial data include more full information than an unfolding function. The reason is that structures are smoothed out (if there are some that are not clear beforehand) due to the finite number of points in the process of discretization of the energy scale if the step is comparable with the structure widths.

In the bremsstrahlung technique a possibility to resolve structures with the

width 200 – 600 keV at a half-maximum for the endpoint step $E_{\gamma max}$ about 50 keV is approximately the same as for the technique of quasimonoenergetic photons with the width 140 – 200 keV at a half-maximum. The differences between these techniques lie in the smoothness of the cross sections and the degree of the structure resolution, which is important for future analysis.

To determine the absolute values of the cross section we used the same scaling factor as for ^{142}Nd which was obtained from the comparison of the maximum of the cross section of our data for ^{142}Nd, measured under the same conditions as ^{208}Pb, with the calculated cross section with the Lorentz distribution parameters from Ref. [22]. A correction on the $\sigma(\gamma,2n)$ contribution was determined according to the statistical theory [23] with a level density parameter obtained from fitting of partial cross sections $\sigma(\gamma,n)$ and $\sigma(\gamma,2n)$ from Ref. [24].

4 Analysis of cross sections and extraction of parameters

For interpretation of the experimental cross section we need a quantitative information which can be compared with the information obtained from other measurements or some theoretical calculations. There are several possibilities of the presentation of results depending on the main goal of the subject.

First, the cross section can be approximated by a Lorentz curve (or two Lorentz curves if we are dealing with the case of statically deformed nuclei), and fitting the data we obtain the parameters of this curve. In this case all intermediate structures are ignored. Such systematic of Lorentz parameters for the cross sections obtained by the quasimonoenergetic photon technique was suggested in Ref. [3]. These parameters can be used for the following de-

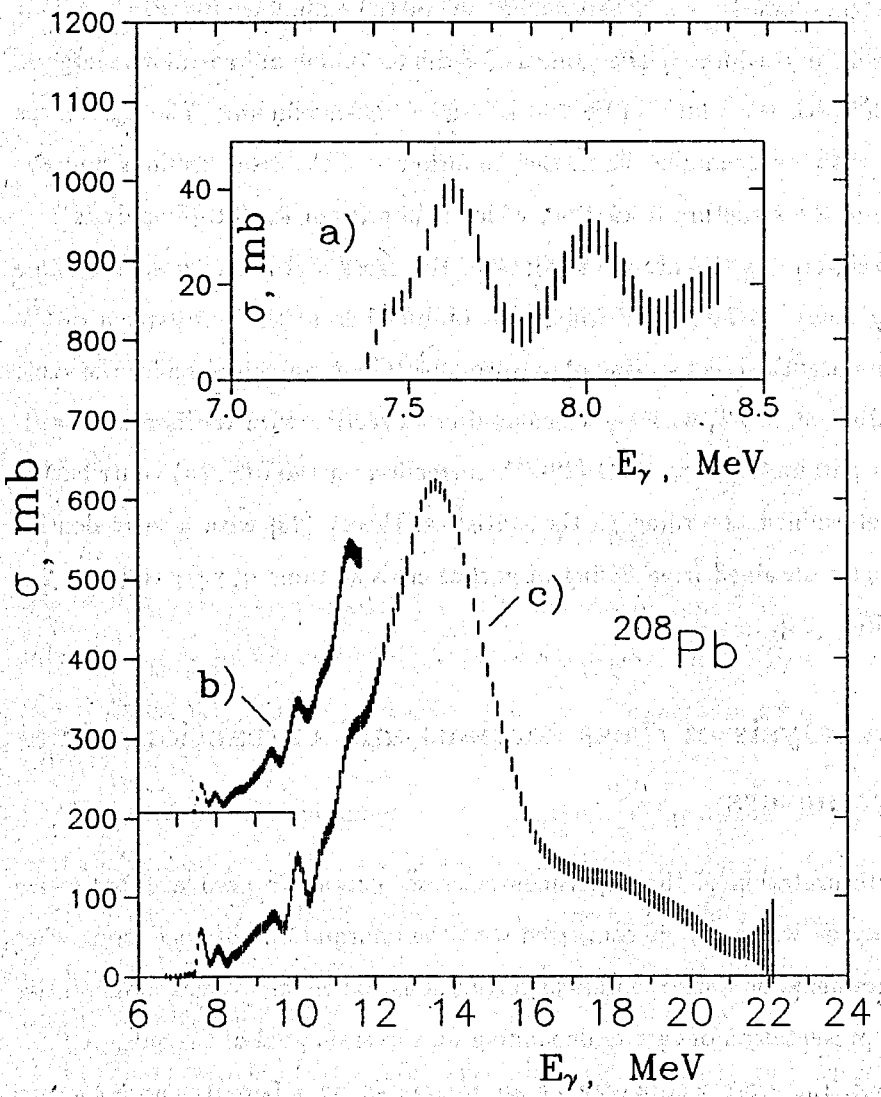

Figure 1: $(\gamma,n)^{208}Pb$ cross section: a) with the step 25 keV [5]; b) with the step 50 keV [5]; c) with the step 40 keV from B_n to 8.5 MeV, with the step 60 keV from 8.5 to 12 MeV and with the step 120 keV from 12 to 22 MeV.

termination of empirical formulae of the GDR location and width in spherical and deformed nuclei as, e.g., in Ref. [25].

Second, the cross section is presented as a superposition of several line sets a type of which is determined either by some physical considerations or by real features of a curve studied. We assume that the GDR is not the single collective state with the width 4 – 6 MeV but a superposition of many resonances with smaller widths located at different energy ranges. If we know the structure characteristics, we can reveal their locations and estimate their contribution to the integral cross section.

The cross section of $(\gamma,n)^{208}Pb$ has well determined structures on the low-energy tail of the GDR and thus, the second method of the developing of information is much more informative. Only energy positions of these structures, given in Refs. [6,24–26], are less useful for a comparison with theoretical calculations.

The experimental (γ,n) cross sections considered in this paper are presented in Fig. 1. This figure shows that the shape and contribution of different structures (even the presence of some of them like the poorly resolved level near 7.43 MeV) of the results obtained with a different step of $E_{\gamma max}$ depends on the resolution and accuracy of measurements.

One can extract a set of parameters which are shown in a table in case of approximating the (γ,n)-cross section by the Gaussian curves

$$\sigma(\gamma,n) = \sum_i \sigma_0^i \exp -[(E - E_0^i)^2/2\delta_i^2] \qquad (3)$$

where $\sigma_0^i, E_0^i, \delta_i$ are the resonance amplitudes, locations and widths forming the cross section, δ_i is the square root of a relevant variance and is related with a half maximum width $\Gamma_i = 2.355\,\delta_i$. Using this set one can obtain relative (in %) and absolute (in mb MeV) contributions of a single peak to the

Table 1: Parameters of decomposition of the $(\gamma, n)^{208}Pb$ cross section by Gaussian curve sets and contribution of each resonance to the integral cross section.

N	σ, mb	E, MeV	δ, MeV	Γ, MeV*	Contr., mb MeV	Contr., %
1	61±2	7.60±0.01	0.095±0.003	0.22	14.3	0.49
2	31±3	8.00±0.02	0.135±0.014	0.32	10.5	0.36
3	31±4	8.64±0.06	0.304±0.026	0.72	23.7	0.81
4	50±4	9.14±0.05	0.235±0.015	0.55	29.3	1.00
5	51±6	9.47±0.03	0.141±0.015	0.33	17.9	0.61
6	133±3	10.03±0.02	0.215±0.018	0.51	71.7	2.45
7	76±22	10.63±0.03	0.176±0.041	0.41	33.7	1.15
8	179±4	11.33±0.03	0.422±0.076	0.99	189.4	6.47
9	48±15	12.20±0.10	0.260±0.076	0.61	31.0	1.06
10	618±4	13.56±0.02	1.227±0.063	2.89	1902.6	65.00
11	54±4	16.00±0.10	0.834±0.040	1.96	114.0	3.86
12	117±3	18.20±0.08	1.688±0.044	3.98	494.7	16.90

integral cross section. The last one is calculated as a sum of squares under the Gaussian curves.

5 Comparison with the theory

The theoretical calculations have been performed within the QPM developed in refs. [14–16]. The wave function of an excited state with taking into account the coupling between the simple (one-phonon) and complex (two-phonon) configurations has the following form:

$$\Psi_\nu(JM) = \{\sum_i R_i(J\nu)Q^+_{JMi} + \sum_{\lambda i\,\lambda' i'} P^{\lambda' i'}_{\lambda i}(J\nu)\left[Q^+_{\lambda\mu i}Q^+_{\lambda'\mu' i'}\right]_{JM}\}\Psi_0 \quad (4)$$

where $Q^+_{\lambda\mu i}$ is the phonon creation operator and ν is the number of excited state, Ψ_0 is the phonon vacuum. The phonon characteristics are determined from the RPA equations. The equations defining the energies $\eta_{J\nu}$ of the state (4) and the quantities R and P are given in ref. [16]. For the intermediate and high excitation energies where the level density is high, it is reasonable to calculate the corresponding strength function

$$b(\Phi,\nu) = \sum_\nu \mid \Phi_{J\nu} \mid^2 \frac{1}{2\pi}\frac{\Delta}{(\eta-\eta_{J\nu})^2+\Delta^2/4}\,, \quad (5)$$

Here $\Phi_{J\nu}$ is the amplitude of the excitation of the state (4) in a nuclear reaction, Δ is the averaging energy interval. It is worth mentioning that a strength function is essentially the same as a response function (see ref. [16]).

The nuclear photoabsorption cross sections are related with a strength function. For example, the energy averaged cross section of the dipole photon adsorption can be written as

$$\sigma_{\gamma t}(E_\gamma) = 4,025\,E_\gamma\, b(E1, E_\gamma) \quad (6)$$

where $\sigma_{\gamma t}$ in mb, E_γ is the photon energy in MeV, $b(E1, E_\gamma)$ in e^2fm^2.

All calculations have been performed with the code GIRES [28]. We used the Saxon–Woods potential with the set of parameters from our previous paper [29] which is a modification of the set from ref. [30]. The single–particle spectrum was fitted to reproduce within the QPM experimental data for the energies, transition probabilities and spectroscopic factors for low lying states of ^{208}Pb and neighboring odd nuclei [29]. The constants of the dipole-dipole force and multipole–multipole forces with the Bohr–Mottelson radial dependence were chosen during a fitting procedure. The ratio of the isoscalar to the isovector constants has been fixed so as to describe the experimental position of the GDR. Our single–particle spectrum included all quasibound states with the orbital momenta $l \leq 9$. A good description of the transition probabilities without any effective charges confirms the completeness of our basis. Our calculations of the integral characteristics of giant resonances in ^{208}Pb [31,32] are in very good agreement with other calculations [9,12] taking the single–particle continuum into account exactly.

Let consider the theoretical description of the GDR integral characteristics in ^{208}Pb. For the energy interval 10.0–17.0 MeV we obtained the following values for the energy centroid $\bar{E}_x = 13.35$ MeV, width $\Gamma = 3.5$ MeV and the energy weighted sum rule (EWSR) is exhausted by 80 % (we have used the value $\Delta = 1.0$ MeV). The experiment [3] gives $\bar{E}_x = 13.46$ MeV, $\Gamma = 3.9$ MeV and the EWSR is exhausted by 89 %. One can see from Fig. 2 a rather good agreement of experimental data with the theoretical calculations for the photoneutron cross section. Some overestimation of a cross section near a maximum and underestimation of a high energy part in our calculation are caused by the truncation of a large number of two phonon states which are weakly coupled with one phonon states. An integral contribution of these components may be essentially taken into account by increasing the energy

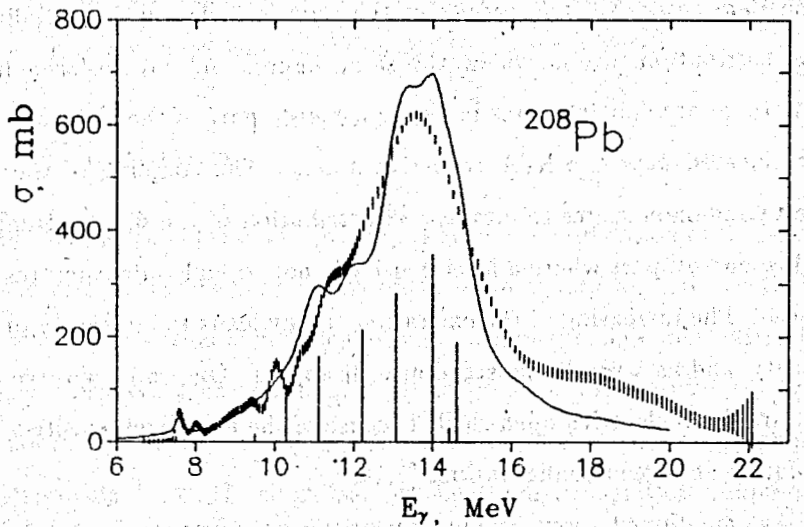

Figure 2: Experimental (dots) and theoretical (solid curve, $\Delta = 1$ MeV) $(\gamma,n)^{208}Pb$ cross sections. Calculation within the RPA in arbitrary units is presented by vertical lines.

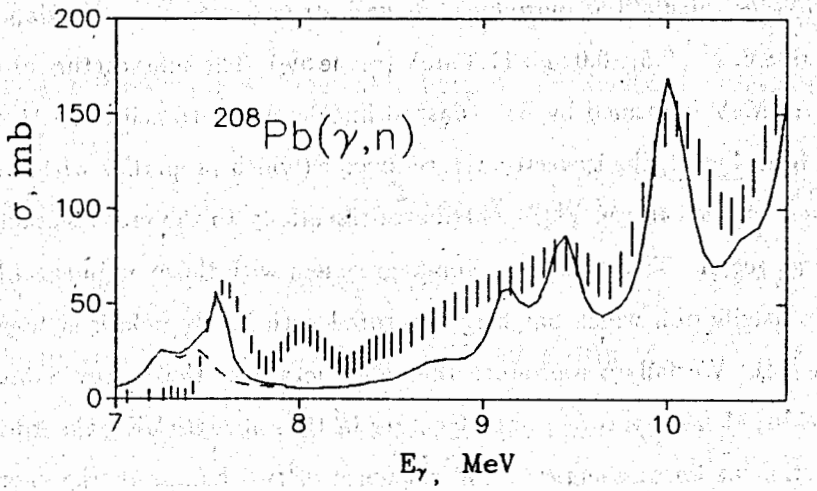

Figure 3: Low–energy part of the $(\gamma,n)^{208}Pb$ cross section (dots – experiment, solid curve – the sum of E1– and M1– photo absorption calculated with $\Delta =$ 0.2 MeV.

averaging parameter Δ. The results of the RPA calculation for the dipole strength distribution are shown in the same figure. As can be seen from Figs. 1,2, there are substructures in the low energy part of the cross section. They are located near the RPA collective states. The coupling of the last with the two phonon states results in a redistribution of the dipole strength. For the low energy part where a level density is not so high substructures are pronounced. The increasing of the excitation energy leads to increasing of the level density, and as a result, substructures disappear. One can't observe any substructures in nuclei with open shells because of the high level densities and strong coupling between configurations [7,16].

As it was mentioned above, the most pronounced substructures take place in the low energy GDR tail (see Fig. 3). To shed more light on the problem of the substructure existence the low energy part of the cross section with smaller $\Delta = 0.2$ MeV has been calculated. The results of calculations are given in Fig. 3. Our calculations reproduce the main structures at the excitation energies 7.6, 8.6, 9.1, 9.5, 10.0 and 11.3 MeV (see table). The substructure at the energy 7.6 MeV is formed by E1- (dashed line) and M1-transitions. As can be seen from Fig. 3, the isovector M1-resonance (which properties within the QPM were studied in ref. [33]) contributes essentially to the cross section in this energy region. This result is in good agreement with the experimental M1 strength distribution which has been measured with highly polarized tagged photons [34]. We fail to reproduce the substructure at the energy 8 MeV, nevertheless, there is a two-bump structure in the calculated E1-absorption cross section at lower energies. The existence of two bumps in the energy interval 7-8 MeV was predicted in our old calculations [7] too. Some disagreement between calculations and experimental data may be caused apparently by inaccuracies of our single particle energies but we didn't try to get an ideal

description of experimental data. It is worth mentioning that E2-transitions don't give any noticeable contribution to the cross section.

6 Conclusion

One can conclude from our investigation that identification of the intermediate structures in the low energy part of the photoabsorption cross section in ^{208}Pb is reliable. Microscopical calculations reproduce rather well particularities of the experimental cross sections. It is possible to interpret the energy dependence of this cross section as a consequence of a ununiform dipole strength distribution due to the single particle shell structure and the coupling between collective and noncollective degrees of freedom in ^{208}Pb.

References

[1] Goeke K., Speth J. Ann. Rev. Nucl. Part. Sci., 1982, v.32, p.65.

[2] Van der Woude A. Progress in Particle and Nuclear Physics, 1987, v.18, p.217.

[3] Berman B.L., Fultz S.C. Rev. Mod. Phys., 1975, v.47, p.713.

[4] Belyaev S.N. et al. Izv. Akad. Nauk SSSR (ser. fiz.), 1984, v.48, p.1940.

[5] Belyaev S.N. et al. Yad. Fiz., 1985, v.42, p.1050.

[6] Van der Vyver R. et al. Z. Phys., 1978, v.A284, p.91.

[7] Soloviev V.G. et al. Nucl. Phys., 1978, v.A304, p.503.

[8] Soloviev V.G. et al. Nucl. Phys., 1977, v.A288, p.376.

[9] De Haro et al. Nucl. Phys. 1982., v.A388, p.265.

[10] Bertsch G. et al. Rev. Mod. Phys., 1983, v.55, p.287.

[11] Tkachev V.N., Kamerdjiev S.P. Yad. Fiz., 1985, v.42, p.832.

[12] Palchik V.V. et al. Yad. Fiz., 1981, v.34, p. 903; 1982, v.35, p.1374.

[13] Bondarenko V.I., Urin M.G. Yad. Fiz., 1987, v.46, p.1068.

[14] Soloviev V.G. Part. and Nucl., 1978, v.9, p.580.

[15] Vdovin A.I., Soloviev V.G. Part. and Nucl., 1983, v.14, p.237.

[16] Voronov V.V., Soloviev V.G. Part. and Nucl., 1983, v.14, p.1381.

[17] Bogdankevich O.V., Nikolaev F.A. Bremsstrahlung technique, M., Atomisdat, 1964.

[18] Belyaev S.N. et al. Pribory i techn. eksperim., 1980, v.1, p.18; 1981, v.1, p.21.

[19] Belyaev S.N. et al. Problems of theoretical nuclear physics, Saratov, SGU, 1982.

[20] Belyaev S.N. et al. Proc. 32 Nucl. Spectr. and Nucl. Struc. Conf., L., Nauka, 1982, p.370.

[21] Turchin V.F. et al. Usp. Fiz. Nayk, 1970, v.102, p.345; Dock. Akad. Nauk SSSR, 1973, v.212, p.561.

[22] Carlos P. et al. Nucl. Phys., 1971, v.A172, p.437.

[23] Blatt J.M., Weisskopf V.F. Theoretical Nuclear Physics, Wiley, New York, N.Y., 1952.

[24] Veyssiere A. et al. Nucl. Phys., 1970, v.A159, p.91.

[25] Carlos P. et al. Electromagnetic interactions of nuclei at low and intrmediate energies, M., Nauka, 1976.

[26] Harvey R.R. et al. Phys. Rev., 1964, v.136, p.B126.

[27] Ichkhanov B.S. et al. Yad. Fiz., 1970, v.12, p.682.

[28] Ponomarev V.Yu. et al. Preprint JINR P-4-81-704, Dubna, 1981.

[29] Voronov V.V., Dao Tien Khoa Izv. Akad. Nauk SSSR (ser. fiz.), 1984, v.48, p.2008.

[30] Chepurnov V.A. Yad. Fiz., 1967, v.16, p.955.

[31] Voronov V.V. et al. Yad. Fiz., 1990, v.51, p.79.

[32] Voronov V.V., Ponomarev V.Yu. Nucl. Phys., 1990, v.A520, p.619c.

[33] Dao Tien Khoa et al. Preprint JINR E-4-86-198, Dubna, 1986.

[34] Laszewski R.M. et al. Phys. Rev. Lett., 1988, v. 61, p.1710.

Received by Publishing Department
on July 5, 1991.